Supporting Information

A Direct Mechanism of Ultrafast Intramolecular Singlet Fission in Pentacene Dimers

Eric G. Fuemmeler[†,#], Samuel N. Sanders[‡,#], Andrew B. Pun[‡,#], Elango Kumarasamy[‡], Tao Zeng[†], Kiyoshi Miyata[‡], Michael L. Steigerwald[‡], X.-Y. Zhu[‡], Matthew Y. Sfeir[§,], Luis M. Campos[‡,*], and Nandini Ananth[†,*]*

[†]Department of Chemistry and Chemical Biology, Cornell University, Ithaca, New York, 14853, USA.
[‡]Department of Chemistry, Columbia University, New York, NY 10027, USA.
[§]Center for Functional Nanomaterials, Brookhaven National Laboratory, Upton, NY 11973, USA.

Table of Contents

1. General Methods

Global Analysis. Global (singular value decomposition-based) and target (differential equation-based) analysis were performed with the Glotaran software package (http://glotaran.org).[1] These methods yield accurate fits of rate constants because they treat the full data set in aggregate. A simple sequential decay model ($S_1 \rightarrow T_1 \rightarrow S_0$) was sufficient to accurately reproduce the data sets obtained for all compounds reported in this manuscript.

Triplet Photosensitization. Triplet photosensitization experiments were used to assign the triplet states in bipentacene compounds (Section S3). Triplets were generated by excitation at 360 nm using a pulse fluence below 100 μJ/cm^2 in a solution of ~20 mM anthracene and ~ 50 μM bipentacene in chloroform. The anthracene directly absorbs the incident photons and undergoes intersystem crossing (ISC) to generate individual triplets. The anthracene triplets were subsequently transferred via diffusional collisions to the bipentacene. An optical probe pulse reveals the induced absorption spectrum of this triplet state and the native triplet lifetime. This method can be contrasted with direct optical excitation, which produced a triplet pair in the case of SF materials.

Photoluminescence Upconversion Spectroscopy. Ultrafast photoluminescence (Section S7) was measured by the upconversion technique. Briefly, a ~100 μM solution in chloroform was resonantly excited with 560 nm, 100 fs laser pulse. Sum frequency generation was achieved by mixing the spontaneous emission with a "gate" pulse in a nonlinear crystal. The magnitude of the unconverted optical signal was proportional to the instantaneous photoluminescence intensity and was measured at intervals of delay between excitation and gate pulse. The spectral resolution of this measurement was ~10 nm, and cross correlation of scattered light from the excitation pulse with the optical gate pulse found a time resolution of ~250 fs.

2. Theory

Truncation of the TIPS Group: Electronic structure calculations reveal that from an orbital viewpoint, the triple bond is the only active portion of the TIPS group (see Figure S1). As such, truncation of the TIPS group to include only acetylene offers substantial computational savings without introducing significant error. A similar conclusion was reached by Kaur *et al*. while studying the effects of substituents in modifying the electronic structure of pentacene moieties.[2]

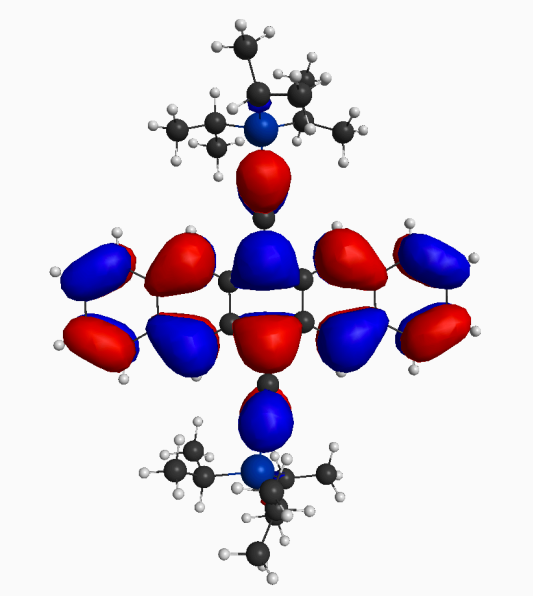

Figure S1. The HOMO of the TIPS-pentacene monomer showing minimal character on the tri-isopropylsilyl groups. Low-lying orbitals of interest show similar distribution across the monomer.

Normal Mode Analysis. The geometric distortions associated with the relaxation from the monomer ground state geometry to optimized T_1 and S_1 geometries are projected onto the excited state normal modes of the substituted pentacene monomer. These normal modes are calculated at the TDDFT/B3LYP level using the 6-31G** basis set.[3,4] The displacement, relaxation energy and Huang-Rhys factor are calculated for each mode and relaxation pathway as shown in Tables S1 & S2. The Huang-Rhys factor is a measure of a mode's vibrational coupling to an electronic transition and is given by $S_i = \frac{\omega_i Q_i^2}{2\hbar}$ where ω_i and Q_i denote the *i*th mode's frequency and displacement, respectively. We identify the mode near 1435 cm^{-1} as the dominant mode in each case, ruling out the low frequency mode near 258 cm^{-1} due to its small relaxation energy. We note that other modes most notably one with frequency ~1250 cm^{-1} may be significant and will be considered in future work.

Table S1. Monomer normal mode analysis of the relaxation from S_0 to S_1.

Frequency (cm^{-1})	Displacement	Relaxation Energy (eV)	Huang-Rhys Factor
258.27	-0.177476	0.003863	0.120645
384.91	-0.013686	0.000051	0.001069
618.13	0.044277	0.001377	0.017972
686.44	-0.064420	0.003596	0.042248
808.80	-0.066978	0.005396	0.053810
1053.01	-0.022080	0.000994	0.007613
1077.80	0.014811	0.000469	0.003506
1186.91	0.056577	0.008291	0.056345
1249.88	-0.091255	0.023920	0.154361
1400.90	0.067828	0.016601	0.095582
1434.98	0.086064	0.028045	0.157634
1519.31	-0.027047	0.003105	0.016483
1548.22	0.062341	0.017129	0.089234
1592.35	-0.022252	0.002308	0.011693

Table S2. Monomer normal mode analysis of the relaxation from S_0 to T_1.

Frequency (cm^{-1})	Displacement	Relaxation Energy (eV)	Huang-Rhys Factor
258.27	-0.274284	0.009227	0.288159
384.91	0.028754	0.000225	0.004720
618.13	0.028171	0.000558	0.007275
686.44	-0.030436	0.000803	0.009431
808.80	-0.070252	0.005936	0.059200
1053.01	-0.015454	0.000487	0.003729
1077.80	0.016900	0.000610	0.004565
1186.91	0.057338	0.008516	0.057871
1249.88	-0.114775	0.037839	0.244184
1331.11	-0.026976	0.002371	0.014365
1400.90	0.044943	0.007289	0.041965
1434.98	0.115998	0.050945	0.286352
1519.31	-0.052725	0.011799	0.062638
1548.22	0.084727	0.031639	0.164830
1592.35	-0.015619	0.001137	0.005761
2165.82	-0.012865	0.001427	0.005316

PCM Calculation. The results of the shifted CASSCF/PCM(water) calculation using a minimal active space as described in the *Calculation Details* are shown in Table S3.

Table S3. Comparison between diabatic energies calculated at the 4o4e level of theory *in vacuo* and using a polarizable continuum model of water.

Diabatic State	*In Vacuo* Energy (eV)	PCM Energy (eV)
tt	1.31	1.32
ge	1.45	1.47
eg	1.46	1.47
gd	1.59	1.60
dg	1.58	1.60
ac	2.51	2.55
ca	2.56	2.55

3. Triplet Photosensitization

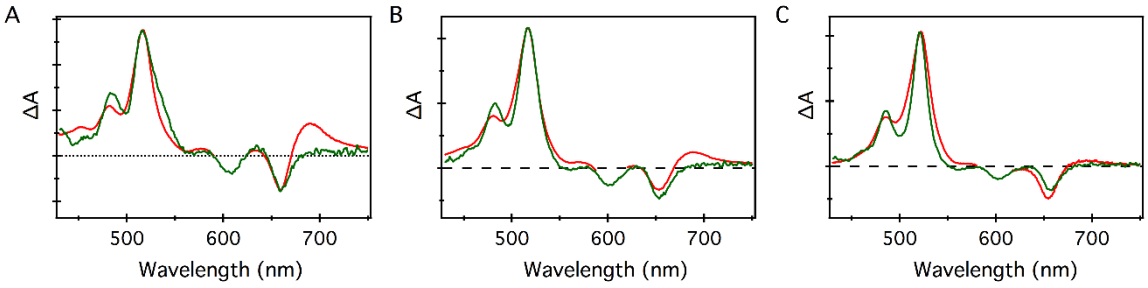

Figure S2. Comparison of the spectra produced by direct photoexcitation (red) and photosensitization by triplet transfer from anthracene for BP-2H (a) BP-HPh (b) and BP-2Ph (c)

The spectrum produced by photoexcitation of the bipentacenes is compared to the spectrum of a single triplet which is populated via triplet transfer from a sensitizer triplet in the photosensitization experiment. Small discrepancies are clearly visible, particularly on the longer wavelength side of the bleach near 700 nm in the less twisted compounds. While the spectra match well, particularly in the more twisted compounds, confirming that it is indeed triplets produced, these modest spectral differences between the one triplet (sensitization) and triplet pair (fission) spectra preclude an effective cross sectional yield determination. Because of the spectral mismatch, the yield determined by a cross sectional calculation would vary depending on the wavelength chosen for the comparison. Instead, we find it more accurate to determine the yield by quantifying the area of the bleach signal before and after fission, as detailed below.

4. Solvent Studies

Shown below are the spectra of singlet and triplet photoinduced absorption (PIA) for BP-HPh as well as kinetic traces from the raw data at the peaks of triplet PIA for the $T_1 \rightarrow T_2$ and $T_1 \rightarrow T_3$ transitions. In addition to these raw kinetic traces, fits obtained from global analysis are overlaid.

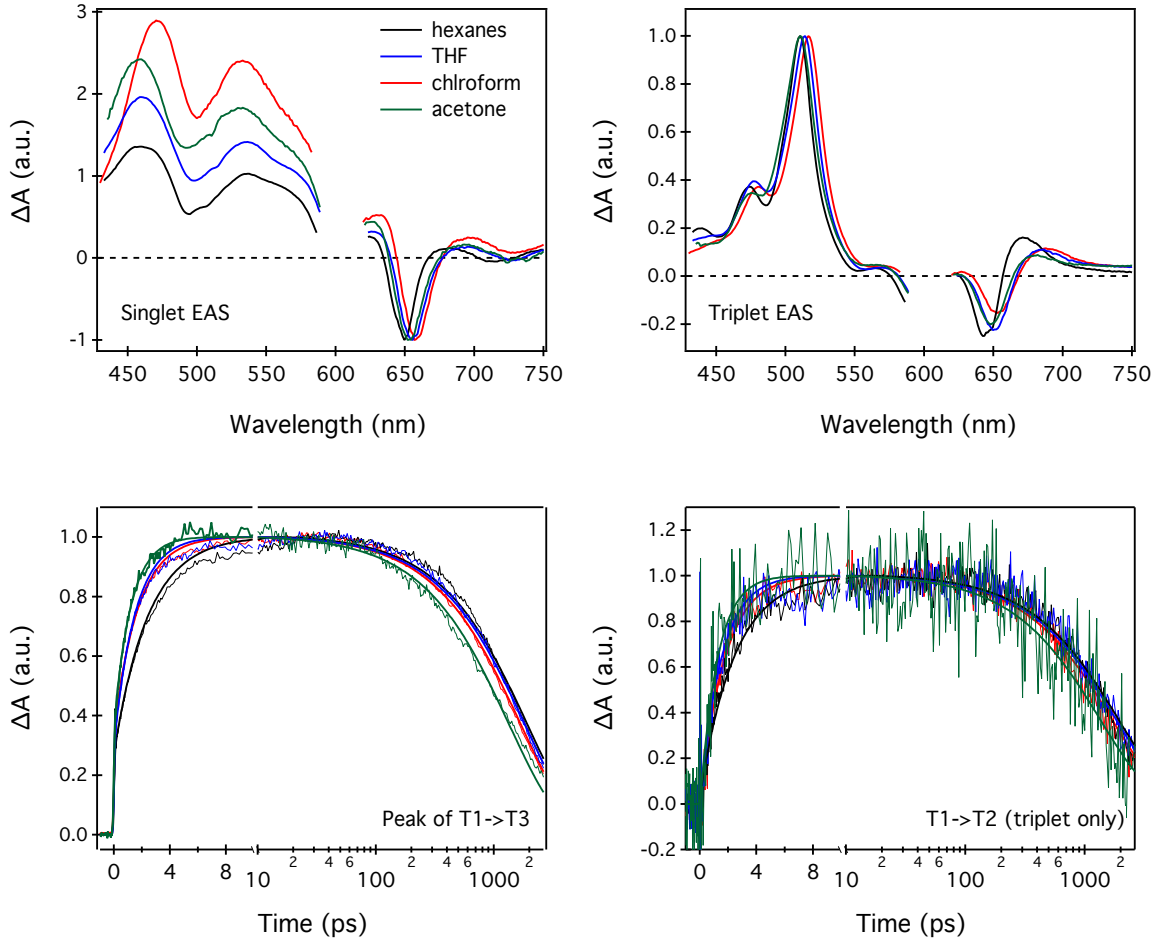

Figure S3. Singlet and triplet spectra solved by singular value decomposition for BP-HPh in a variety of solvents (top) and comparison of fits resulting from global analysis to raw data kinetics at the peak of the triplet PIA bands

The singlet spectra have been normalized to the ground state bleach, which reveals a significant dependence of the oscillator strength of the relative strength of $S_1 \rightarrow S_n$ and the $S_0 \rightarrow S_n$ transitions on solvent as well as a weak solvent dependence of the spectral lineshape. While this solvent dependence reveals a significant effect of the solvent on transitions within the singlet manifold, there is no clear trend based on solvent dielectric constant, refractive index or orientation polarizability.

Similarly, there is some solvent dependence of the triplet PIA. Both the oscillator strength relative to the $S_0 \rightarrow S_n$ transition and the location of the $T_1 \rightarrow T_2$ and $T_1 \rightarrow T_3$ transitions change within solvents. For example, the $T_1 \rightarrow T_2$ transition red shifts as the solvent is changed from acetone to

hexanes to THF to chloroform. Again, these shifts do not follow a clear trend based on solvent dielectric constant or other factors, but reveal a significant and complex effect of solvent on transitions among states within the triplet manifold.

Pertinent kinetic information obtained from global analysis is summarized in the table below. Also included is solvent information which might be expected to systematically affect fission rate in the case of a CT mediated process.

Table S4. Summary of fission rate constants, triplet pair decay time constants, and wavelength of maximum absorption for BP-HPh in different solvents, compared with ε (solvent dielectric), n (index of refraction) and Δf (orientation polarizability).

Solvent	Fission Rate constant (ps^{-1})	TT Decay Rate constant (ps^{-1})	Abs. Max (nm)	ε	n	Δf
Hexanes	0.41	5.2×10^{-4}	646	1.9	1.375	1.2×10^{-3}
Chloroform	0.58	6.0×10^{-4}	654	4.8	1.446	1.5×10^{-1}
THF	0.65	5.5×10^{-4}	652	7.5	1.407	2.1×10^{-1}
Acetone	0.81	7.4×10^{-4}	650	21	1.359	2.8×10^{-1}

The triplet pair decay rate has significant but complex dependence on solvent, with the fastest decay in acetone 1.42 times the rate of decay in hexane. However, this triplet pair lifetime is not strictly solvent dielectric constant or orientation polarizability dependent, as the lifetime in chloroform exceeds that in THF. This dependence suggests that the nature of the triplet pair state produced by fission is affected by the choice of solvent. This change in the nature of the final state produced by fission suggests that the conversion from singlet to triplet pair state should be solvent dependent as well, regardless of fission mechanism.

As summarized in the table, the fission rate for BP-HPh has some modest solvent dependence, which is unsurprising since solvent affects the singlet and triplet energy levels, transition oscillator strengths and triplet pair lifetimes. SF in this particular dimer occurs somewhat faster in solvents with larger dielectric constants and larger orientation polarizability. While this modest dependence might serve as circumstantial evidence for the involvement of CT states in SF for this dimer, the complex relationship of the singlet and triplet state energies and oscillator strengths on solvent suggest that the situation is complex, and other factors could explain such a solvent dependence without necessitating CT states. More succinctly, while CT mediated fission would certainly result in some solvent dependence of fission rates, some solvent dependence does not necessarily imply CT mediated fission.

Shown below is the singlet and triplet PIA for BP-2Ph, the most twisted dimer studied in this work. In the bottom of the figure, kinetic traces from raw data are compared to fits obtained from global analysis.

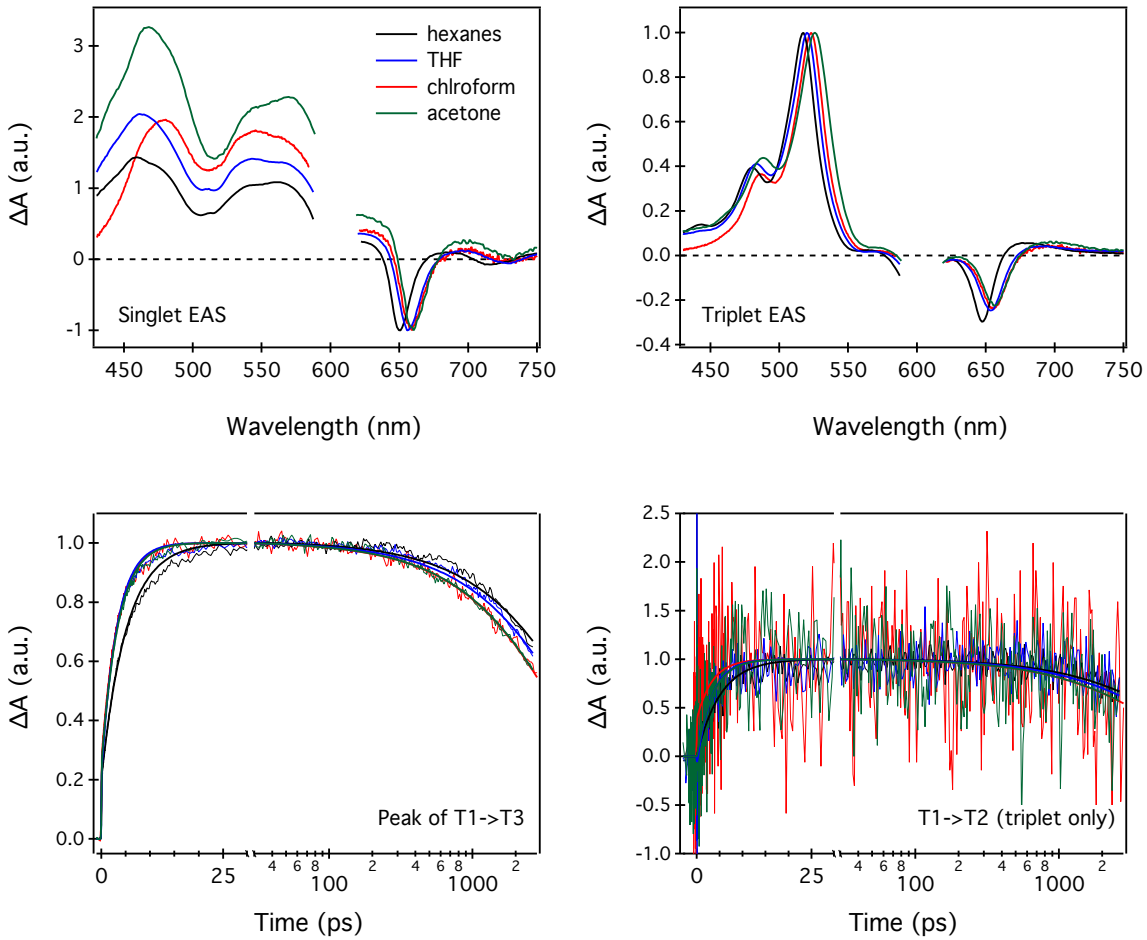

Figure S4. Singlet spectra solved by singular value decomposition for BP-HPh in a variety of solvents (top) and comparison of fits resulting from global analysis to raw data kinetics at the peak of the triplet PIA bands

Again, we observe strong solvent dependence of the relative oscillator strengths of the $S_1 \rightarrow S_n$ and $S_0 \rightarrow S_n$ transitions and modest dependence of the energy of these transitions. Again, there is no clear trend based on solvent dielectric constant, index of refraction or orientation polarizability. Similarly, the energies and oscillator strengths of the transitions within the triplet manifold are also solvent dependent.

Table S5. Summary of fission rate constants, triplet pair decay time constants, and wavelength of maximum absorption for BP-2Ph in different solvents, compared with ε (solvent dielectric), n (index of refraction) and Δf (orientation polarizability).

Solvent	Fission Rate Constant (ps^{-1})	TT Decay Rate Constant (ps^{-1})	Abs. Max (nm)	ε	n	Δf
Hexanes	0.19	1.6×10^{-4}	649	1.9	1.375	1.2×10^{-3}
Xylene	0.29	1.8×10^{-4}	657	2.6	1.505	2.9×10^{-2}
Chloroform	0.30	2.2×10^{-4}	657	4.8	1.446	1.5×10^{-1}
THF	0.31	1.8×10^{-4}	655	7.5	1.407	2.1×10^{-1}

In BP-2Ph, we also find the triplet pair decay rate is dependent on solvent. In this case, chloroform has the longest lifetime, 1.38 times longer than the lifetime in the hexanes, the solvent with the fastest triplet pair decay.

In this case, we find SF is again the slowest in hexanes. However, SF is nearly constant between xylenes, chloroform, and THF despite these solvents ranging a factor of 4 in dielectric constant and orders of magnitude in orientation polarizability. While there appears to be some marginal dependence on these two factors, this dependence is within the margin of error for our rate determinations and is much smaller than the type of strong dependence expected for CT mediated fission. In summary, there are significant differences in the solvent dependence of fission even among BP-HPh and BP-2Ph. This varying strength of solvent dependence indicates some system-specific dependence of SF on shifting energy levels and solvation environment, but not the type of systematic and strong dependence which would necessarily implicate CT states in the fission process.

5. Yield Determination

We have previously demonstrated that, in pentacene dimers directly covalently bound at the 2 position, modest differences arise between the triplet spectrum of a single triplet, produced by triplet photosensitization, and the spectrum of a triplet pair, produced by singlet fission (direct photoexcitation).[5] Such differences in the photoinduced absorption of a single triplet and a triplet pair render cross-sectional yield determinations based on the photoinduced absorption inaccurate. Indeed, because of these discrepancies, the yield will vary based on which wavelength is chosen for the determination. While we have also demonstrated that further separation of the pentacenes by a conjugated spacer such as a biphenyl group can converge the one-triplet and triplet pair spectra, allowing for an accurate photoinduced absorption cross-sectional yield, in this manuscript we only present directly-linked pentacene dimers where we again observe modest spectral differences between a single triplet exciton and a triplet pair. Because of this shifting, it is more

accurate to determine the yield based on analysis of the area of the ground state bleach as described below.

We have previously demonstrated that, in BP-2H and related pentacene dimers, the singlet exciton quantitatively bleaches the ground state $S_0 \rightarrow S_n$ transitions. This information can be obtained from power-dependent transient absorption spectroscopy, where the height of the ground state bleach is equivalent to the full value of the ground state extinction coefficient. This analysis can be further confirmed by saturable absorption experiments. Because the singlet exciton bleaches the entire molecule, no ground state absorption can occur on a molecule which is already excited with a singlet exciton. Therefore, saturable absorption measurements show it is not possible to populate a biexciton on these molecules. These results are corroborated by similar measurements on comparable covalent pentacene dimers which lead to similar conclusions.[6] In this manuscript, we confirm that the singlet exciton still bleaches the entire bipentacene even in the more twisted dimers by verifying conservation of the quantity $\frac{\Delta A}{\varepsilon * (1-T)}$ when measuring solutions under identical excitation conditions.

BP-2H:

Optical Density of solution in chloroform at 600 nm (the pump wavelength): 0.304

Bleach minimum: 2.54mOD @ 658

Calculate quantity DA/(e*(1-T))

2.54/(44000*(1-10^-.304)) = 1.15e-4

BP-HPh:

Optical Density of solution in chloroform at 600 nm: 0.332

Bleach minimum: 2.25mOD @ 656

2.25/(36000*(1-10^-.332)) = 1.17e-4

BP-2Ph:

Optical Density of solution in chloroform at 600 nm: 0.254

Bleach minimum: 1.89mOD @ 659

1.92/(43000*(1-10^-.254)) = 1e-4

The agreement, which is well within the margin of error for these calculation when considering both experimental error and error caused by some modest overlap of induced absorption signals with the bleach minimum, confirm that the entire molecule is bleached by the singlet exciton in all three cases. In this case, the bleach before and after singlet fission should be unchanged.

When evaluating the bleach before and after fission, in which case we expect a quantitative yield to have a constant bleach, we find it most accurate to compare the area of the bleach signal, not the height at a given wavelength. Comparing the area corrects to some extent for differences in bleach which are simply caused by overlap with photoinduced absorption of either the singlet or triplet exciton and not a change in overall excited state population.

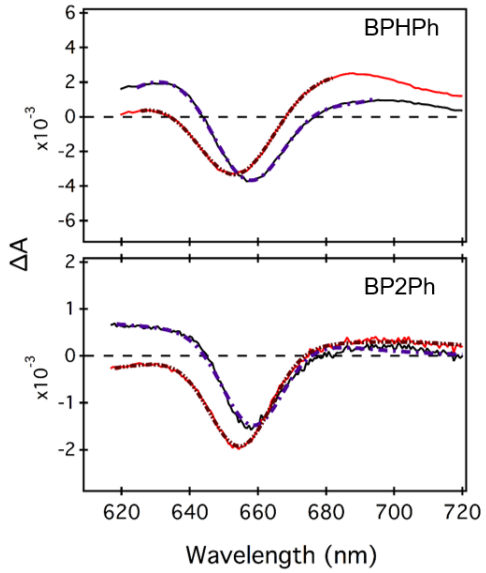

Figure S5: Ground state bleach signal of BP-HPh (above) and BP-2Ph (below) showing fits to the singlet (purple) and triplet pair (red) spectra.

The singlet Gaussian fit to the singlet exciton in BP-HPh gives an area of 71.33(a.u.), in good agreement with the area of the triplet pair bleach after iSF of 79.22(a.u.). Similarly, the singlet exciton fit for BP-2Ph gives an area of 23.3 (a.u.), which is equivalent within our margin of error to the triplet pair bleach area of 25.6 (a.u.). Accounting for the bleach of both pentacene units by a singlet exciton or a triplet pair, this result confirms that these two new dimers also result in quantitative iSF. This result is expected, as iSF occurs in all cases in under 10 ps, a rate drastically faster than competing processes in TIPS-pentacene based chromophores such as intersystem crossing or fluorescence, which both occur on a 10s of ns timescale.[7]

6. Steady-state absorption spectroscopy

Extinction coefficients were determined by UV-Visible steady state absorption spectroscopy of a measured mass of material in a known volume of chloroform. Several concentrations were measured for each bipentacene which confirmed the adherence of these materials to Beer's Law. The resultant plot of extinction coefficient versus wavelength is shown below.

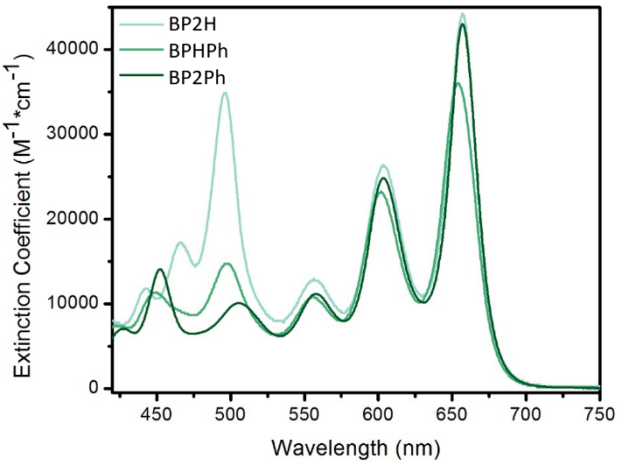

Figure S6: Extinction coefficient versus wavelength of the bipentacenes discussed in chloroform.

Steady state spectra were also obtained for these compounds in a variety of solvents. The location of the λ_{max}, which corresponds to the $S_0 \rightarrow S_1$ transition is summarized for these varied solvents in the tables listed above.

7. Ultrafast Photoluminescence Upconversion Spectroscopy

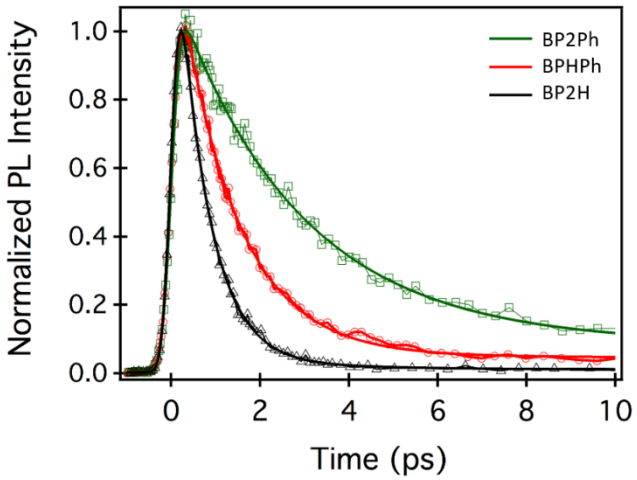

Figure S7: Plotoluminescence upconversion spectroscopy in chloroform reveals the decay of the emissive singlet exciton into the non-emissive two-triplet state.

In singlet fission, a singlet is converted into two triplets. Because a singlet exciton is fluorescent, whereas fluorescence is forbidden for triplet excitons, this process corresponds to conversion of an emissive state into a non-emissive state. Because there are no significant competing processes observed in the bipentacenes presented in this work, the decay of the emissive singlet exciton, followed by upconversion photoluminescence spectroscopy, is equivalent to the singlet fission rate and fitting this photoluminescence decay gives equivalent results to the rates determined by transient absorption spectroscopy.

8. Bond Lengths Determined by Single Crystal X-ray Diffraction

We have previously reported the crystal structure of BP-2H.[5] We have reproduced it below.

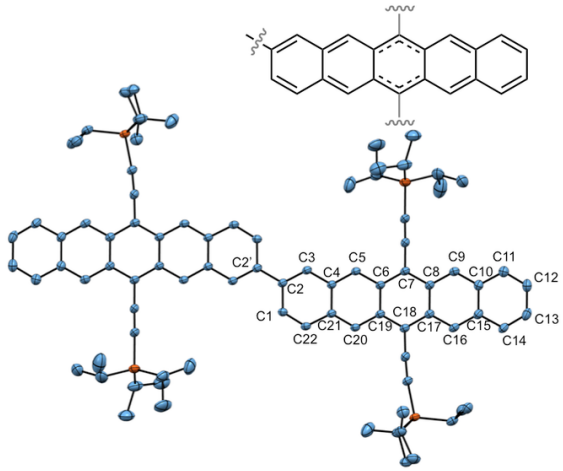

Carbon-carbon distances (double-bond character): C2-C3 & C1-C22 = 1.37Å; C4-C5, C20-C21, C9-C10, C15-C16 = 1.38Å; C11-C12 & C13-C14 = 1.36Å;
(delocalized/single-bond character) C3-C4, C21-C22, C10-C11, C14-C15 = 1.43Å; C5-C6, C19-C20, C6-C7, C18-C19, C7-C8, C17-C18, C8-C9, C16-C17 = 1.41Å; C2-C2' = 1.48Å; C1-C2, C4-C21, C6-C19, C8-C17, C10-C15 = 1.45Å; C12-C13 = 1.43Å.

Figure S8. Structure of BP-2H from single crystal X-ray diffraction.

The full dimer is shown in the ball and stick figure and has the bond lengths listed. From these bond lengths, we can infer the relative single and double bond character, shown in the line diagram for half of the dimer.

9. General Synthetic Methods

All commercially obtained reagents/solvents were used as received; chemicals were purchased from Alfa Aesar®, Sigma-Aldrich®, Acros organics®, TCI America®, Mallinckrodt®, and Oakwood® Products, and were used as received without further purification. Unless stated otherwise, reactions were conducted in oven-dried glassware under argon atmosphere. ^{1}H-NMR and ^{13}C-NMR spectra were recorded on Bruker 400 MHz (100 MHz for ^{13}C) and on 500 MHz (125 MHz for ^{13}C) spectrometers. Data from the ^{1}H-NMR and ^{13}C spectroscopy are reported as chemical shift (δ ppm) with the corresponding integration values. Coupling constants (*J*) are reported in hertz (Hz). Standard abbreviations indicating multiplicity were used as follows: s (singlet), b (broad), d (doublet), t (triplet), q (quartet), m (multiplet) and virt (virtual). The mass spectral data for the compounds were obtained from XEVO G2-XS Waters® equipped with a QTOF detector with multiple inlet and ionization capabilities including electrospray ionization (ESI), atmospheric pressure chemical ionization (APCI), and atmospheric solids analysis probe (ASAP). The base peaks were usually obtained as $[M]^{+}$ or $[M+H]^{+}$ ions.

Anhydrous solvents were obtained from a Schlenk manifold with purification columns packed with activated alumina and supported copper catalyst (Glass Contour, Irvine, CA). All reactions were carried out under argon unless otherwise noted.

General protocol for the synthesis of Bipentacenes:

Synthesis of Dibromo TIPS pentacene:

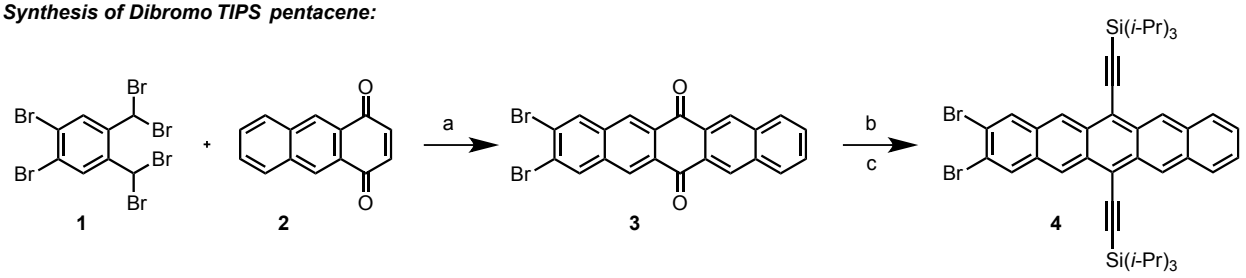

a) DMF, KI, 100 °C, 24 h; b) 1. *n*-BuLi, TIPS-acetylene, THF, -78 to 25 °C , 1 h; c) **3**, rt, 16 h followed by *Satd.* $SnCl_2$ in 10% HCl, 1 h

Synthesis of Bipentacenes:

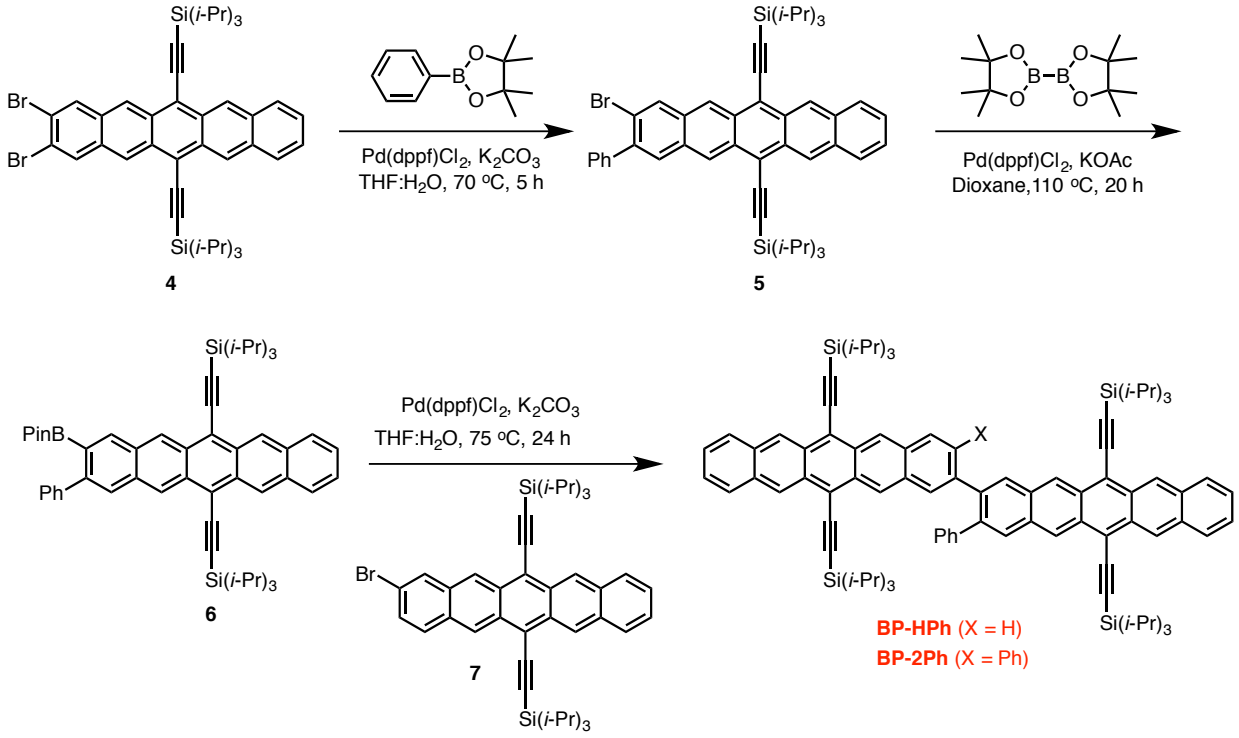

General procedure for the synthesis of pentacenes and its derivatives

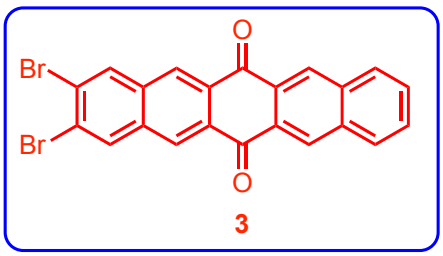

The 6,13-pentacenequinone **3** was synthesized according to a procedure reported in the literature.[8]

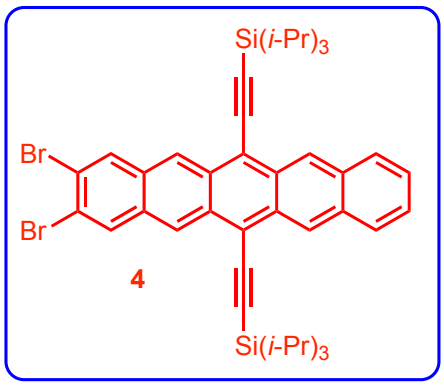

To a solution of triisopropylsilylacetylene (3.5 *equiv*.) in dry and degassed THF (25 mL) in 200 mL Schlenk flask at -78 °C *n*-butyl lithium (3.4 *equiv*., 2.5 M in hexanes) was added. This solution was allowed to warm to room temperature and stirred for 1 h followed by the addition of **3** (4.0 g, 1.0 *equiv*.) under positive argon flow. The solution was allowed to warm to rt and stirred for 16 h or until solid pentacenoquinone was no longer observed. To this clear, deep yellow solution was added of a saturated solution of tin (II) chloride dihydrate in 10% aqueous HCl solution (50 mL) during which the solution turned deep blue. The resulting mixture was stirred at rt for 1 h under dark and filtered over a pad of silica. The solid was washed with DCM and the combined organic layer was washed with water (2 · 200 mL), dried over *anhyd*. Na_2SO_4, filtered and the solvent was removed under reduced pressure to get the crude product. The crude was purified by silica chromatography using hexanes as an eluent to obtain dibromo pentacene as a deep blue solid.

Note: The intermediate diol can be isolated to remove excess TIPS acetylenes prior to the $SnCl_2.H_2O$ reduction, or can be removed under high vacuum after column chromatography.

Yield: 76% (Blue Solid)

^{1}H-NMR (400 MHz, $CDCl_3$, δ ppm): 9.29 (m, 2H), 9.18 (m, 2H), 8.28 (m, 2H), 7.98-7.96 (m, 2H), 7.44-7.42 (m, 2H) and 1.46-1.34 (m, 42H).

^{13}C-NMR (125 MHz, $CDCl_3$, δ ppm): 132.7, 132.6, 131.1, 130.9, 130.7, 128.7, 126.5, 126.4, 125.9, 122.3, 118.8, 108.8, 104.2, 19.0 and 11.7.

MS (ESI): Calculated: 794.1974; Observed: 794.1971.

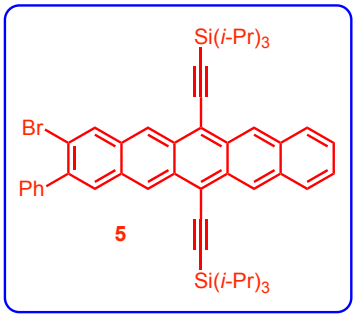

To a dry round bottomed flask was added **4** (1.5 g, 1.88 mmol), $Pd(dppf)Cl_2 \cdot DCM$ (73.5 mg, 0.09 mmol), and phenylboronic acid pinacol ester (349.5 mg, 1.71 mmol). Sequential vacuum and argon were used to degas the mixture followed by the addition of dry THF (45 mL) and K_2CO_3 (2.36 g, 17.1 mmol) in sparged DI water (15 mL). The mixture was then brought to 70 °C and allowed to heat for 5 h. The mixture was cooled to rt and the crude was partitioned between hexanes (250 mL) and water (200 mL). The organic layer was separated, washed with water (2 · 200 mL), and brine (100 mL), dried over *anhyd*. Na_2SO_4, filtered and the solvent was removed under reduced pressure to get the crude product. The crude was purified by silica chromatography using mixtures of hexanes/DCM as an eluent to obtain **5** as a blue solid (632 mg, 42 %)

^{1}H-NMR (400 MHz, $CDCl_3$, δ ppm): 9.31-9.30 (m, 2H), 9.26-9.24 (m, 2H), 8.33 (s, 1H), 7.99-7.95 (m, 2H), 7.89 (s, 1H), 7.59-7.41 (m, 7H) and 1.42-1.32 (m, 42H).

^{13}C-NMR (125 MHz, $CDCl_3$, δ ppm): 140.9, 139.99, 132.5, 132.4, 132.1, 131.9, 130.9, 130.8, 130.1, 129.8, 128.7, 128.0, 127.9, 126.8, 126.5, 126.4, 126.3, 126.2, 125.2, 122.1, 118.6, 107.7, 107.65, 104.5, 104.4, 19.04, 19.02, 11.7 and 11.6.

MS (ESI): Calculated: 792.3182; Observed: 792.3184.

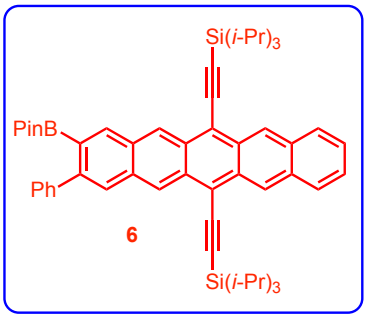

To a dry round bottomed flask was added **5** (600 mg, 0.76 mmol), $Pd(dppf)Cl_2 \cdot DCM$ (61.6 mg, 0.07 mmol), and bis(pinacolato)diboron (384 mg, 1.51 mmol). Sequential vacuum and argon were used to degas the mixture followed by the addition of KOAc (148 mg, 1.51 mmol) in sparged dioxane (21 mL). The mixture was brought to 110 °C and allowed to stir for 20 h in the dark. The mixture was cooled to rt and the solvent was removed under reduced pressure. The crude was partitioned between Hexanes (50 mL) and water (50 mL). The organic layer was separated, washed with water (2 · 50 mL) and brine (25 mL), dried over *anhyd*. Na_2SO_4, filtered and the solvent was removed under reduced pressure to isolate the crude product. The crude was purified by silica chromatography using mixtures of hexanes/DCM as an eluent to obtain **6** as a blue solid (123 mg, 19 %)

^{1}H-NMR (400 MHz, $CDCl_3$, δ ppm): 9.35 (s, 1H), 9.32-9.31 (s, 2H), 9.26 (s, 1H), 8.40 (s, 1H), 7.98-7.96 (m, 2H), 7.90-7.89 (m, 1H), 7.59-7.57 (m, 2H), 7.48-7.38 (m, 5H), 1.42-1.34 (m, 42H) and 1.29 (s, 12H).

^{13}C-NMR (125 MHz, $CDCl_3$, δ ppm): 143.1, 142.7, 137.99, 132.5, 132.4, 132.3, 131.3, 130.8, 130.76, 130.7, 130.6, 129.0, 128.7, 128.0, 127.4, 127.37, 127.1, 127.0, 126.4, 126.3, 126.1, 126.06, 126.0, 118.8, 118.2, 114.9, 107.3, 107.2, 104.7, 104.6, 84.0, 24.7, 19.0, 19.02, 11.7 and 11.6.

MS (ESI): Calculated: 840.4940; Observed: 840.4929.

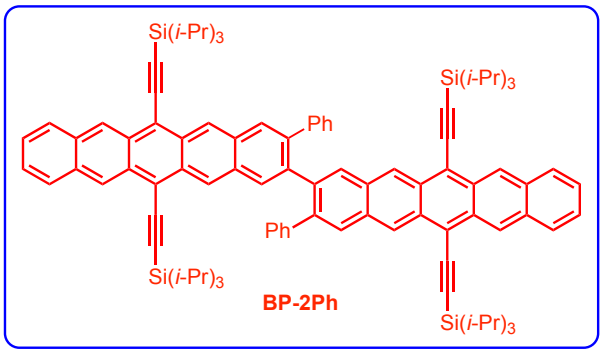

To a flame dried 3 neck RBF was added **7** (50 mg, 0.06 mmol), **6** (56.6 mg, 0.07 mmol) and $Pd(dppf)Cl_2$·DCM (4 mg, 0.005 mmol). Sequential vacuum and argon were used to degas the mixture followed by the addition of degassed dry THF (32 mL) and K_2CO_3 (138 mg, 1.0 mmol) in sparged DI Water (3 mL). The resulting solution was brought to 75 °C and allowed to stir for 24 h in the dark. The solution was poured into a separatory funnel containing DCM (30 mL) and water (30 mL). The organic layer was separated, dried over *anhyd*. Na_2SO_4, filtered and the solvent was removed under reduced pressure to get the crude product. The crude was purified by silica chromatography using mixtures of hexanes/DCM as an eluent to obtain product as a blue-green solid (30 mg, 35 %)

^{1}H-NMR (400 MHz, $CDCl_3$, δ ppm): 9.46 (s, 2H), 9.38-9.37 (m, 4H), 9.32 (s, 2H), 8.34 (s, 2H), 8.04-8.00 (m, 4H), 7.79 (s, 2H), 7.48-7.44 (m, 4H), 7.21-7.16 (m, 2H), 7.09-7.05 (m, 4H), 6.88-6.85 (m, 4H) and 1.47-1.37 (m, 84H).

^{13}C-NMR (125 MHz, $CDCl_3$, δ ppm): 140.6, 140.2, 140.1, 132.4, 132.36, 131.99, 131.7, 131.1, 130.99, 130.95, 130.8, 130.8, 129.2, 129.1, 128.7, 127.7, 126.5, 126.4, 126.2, 126.1, 118.5, 118.4, 107.4, 107.3, 104.7, 104.67, 29.7, 19.1, 19.0, 11.7 and 11.70.

MS (ESI): Calculated: 1426.798; Observed: 1426.7957.

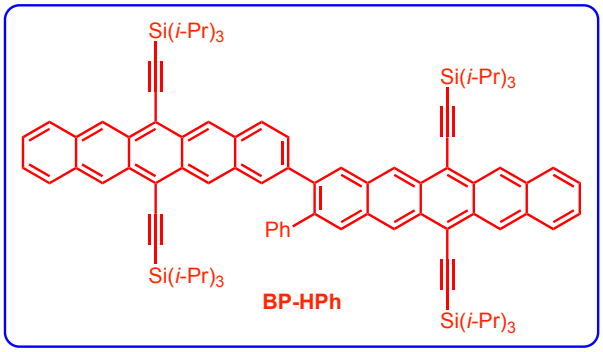

This compound was synthesized following the procedure mentioned above, where compound **5** was coupled with pinacolatoboron TIPS pentacene. We have previously reported the synthesis of this borylated TIPS-Pentacene.[5] Yield = 60 % (Blue-green solid).

^{1}H-NMR (400 MHz, $CDCl_3$, δ ppm): ^{1}H-NMR (500 MHz, $CDCl_3$, δ ppm): 9.42 (s, 1H), 9.37 (s, 1H), 9.34-9.32 (m, 4H), 9.29 (s, 1H), 9.25 (s, 1H), 8.22 (s, 1H), 8.09-8.06 (m, 2H), 8.01-7.98 (m, 4H), 7.79-7.77 (m, 1H), 7.47-7.41 (m, 6H), 7.33-7.28 (m, 3H), 7.19-7.16 (m, 1H) and 1.46-1.35 (m, 84H).

^{13}C-NMR (125 MHz, $CDCl_3$, δ ppm): 141.4, 139.8, 139.7, 139.4, 132.54, 132.53, 132.5, 132.46, 131.9, 131.87, 131.4, 131.2, 131.19, 131.0, 130.9, 130.91, 130.8, 130.78, 130.3, 130.25, 129.9, 128.9, 128.85, 128.84, 128.7, 128.4, 127.9, 127.2, 126.6, 126.58, 126.54, 126.49, 126.4, 126.3, 126.2, 118.7, 118.59, 118.56, 118.4, 107.6, 107.5, 107.4, 107.3, 104.9, 104.8, 19.19, 19.16 and 11.9.

MS (ESI): Calculated: 1350.7685; Observed: 1350.7648.

^{1}H-NMR (400 MHz, $CDCl_3$, δ ppm): 9.29 (m, 2H), 9.18 (m, 2H), 8.28 (m, 2H), 7.98-7.96 (m, 2H), 7.44-7.42 (m, 2H) and 1.46-1.34 (m, 42H).

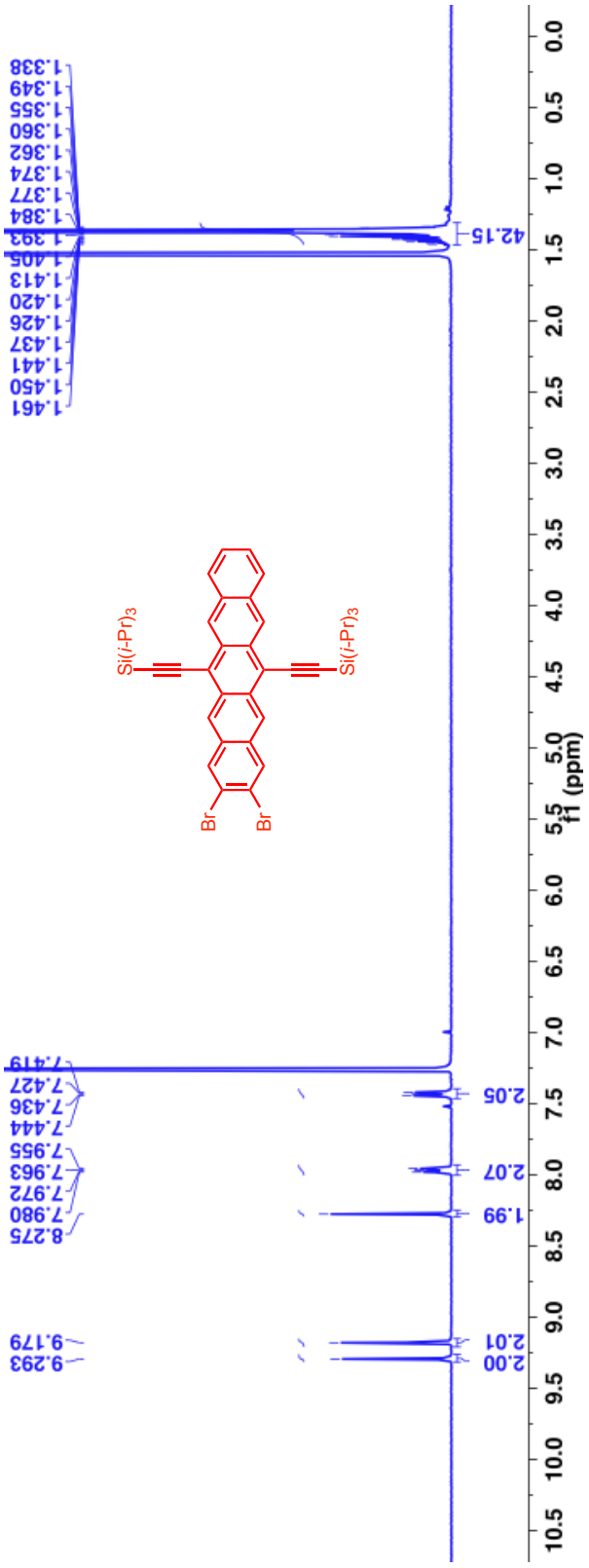

^{13}C-NMR (125 MHz, $CDCl_3$, δ ppm): 132.7, 132.6, 131.1, 130.9, 130.7, 128.7, 126.5, 126.4, 125.9, 122.3, 118.8, 108.8, 104.2, 19.0 and 11.7.

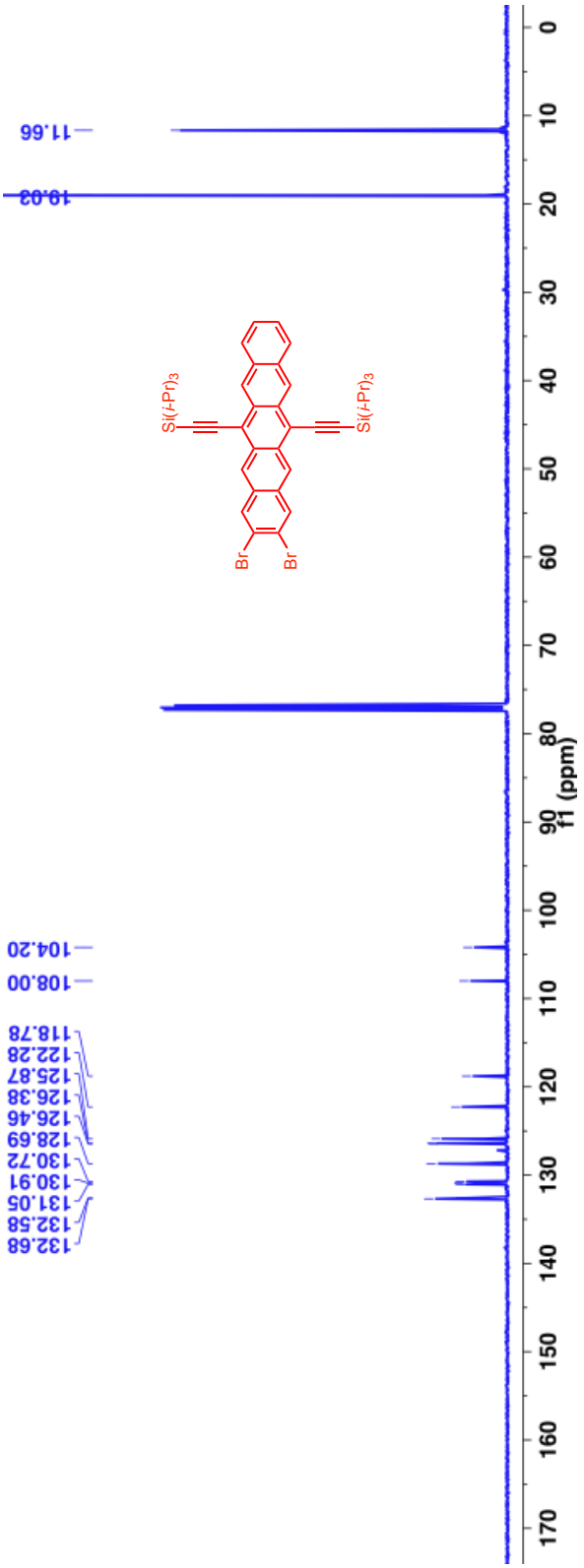

^{1}H-NMR (400 MHz, $CDCl_3$, δ ppm): 9.31-9.30 (m, 2H), 9.26-9.24 (m, 2H), 8.33 (s, 1H), 7.99-7.95 (m, 2H), 7.89 (s, 1H), 7.59-7.41 (m, 7H) and 1.42-1.32 (m, 42H).

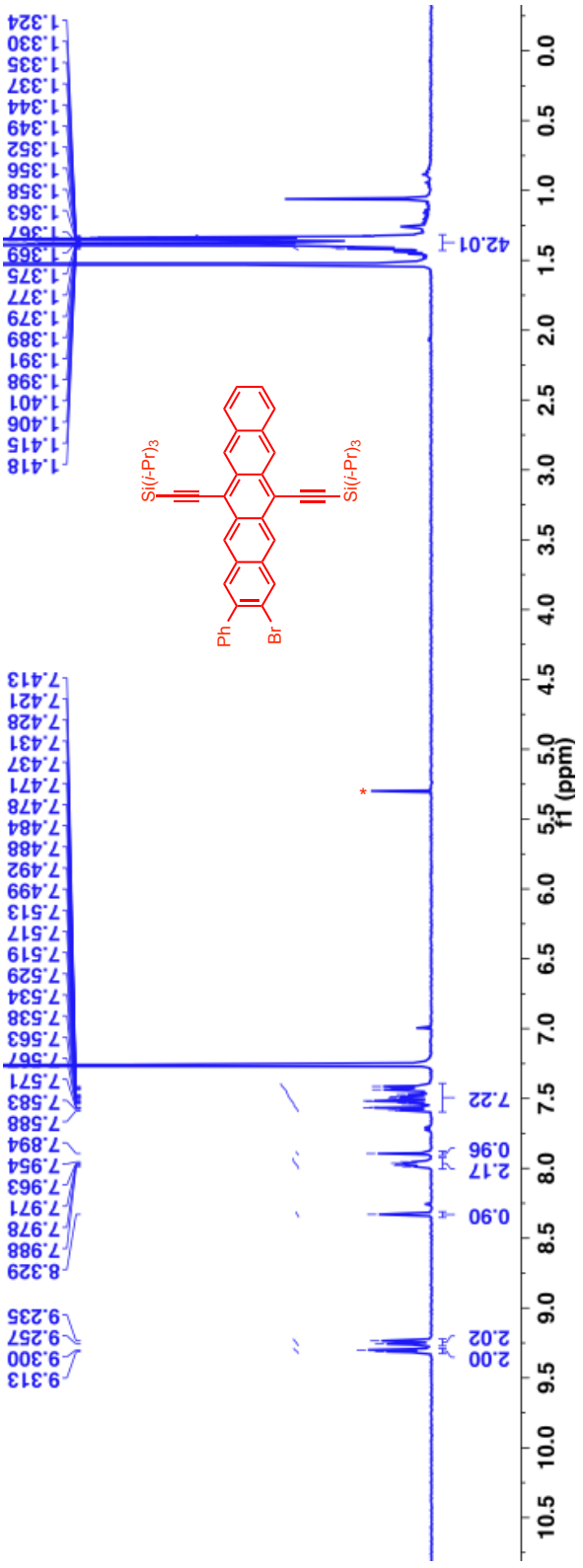

^{13}C-NMR (125 MHz, $CDCl_3$, δ ppm): 140.9, 139.99, 132.5, 132.4, 132.1, 131.9, 130.9, 130.8, 130.1, 129.8, 128.7, 128.0, 127.9, 126.8, 126.5, 126.4, 126.3, 126.2, 125.2, 122.1, 118.6, 107.7, 107.65, 104.5, 104.4, 19.04, 19.02, 11.7 and 11.6.

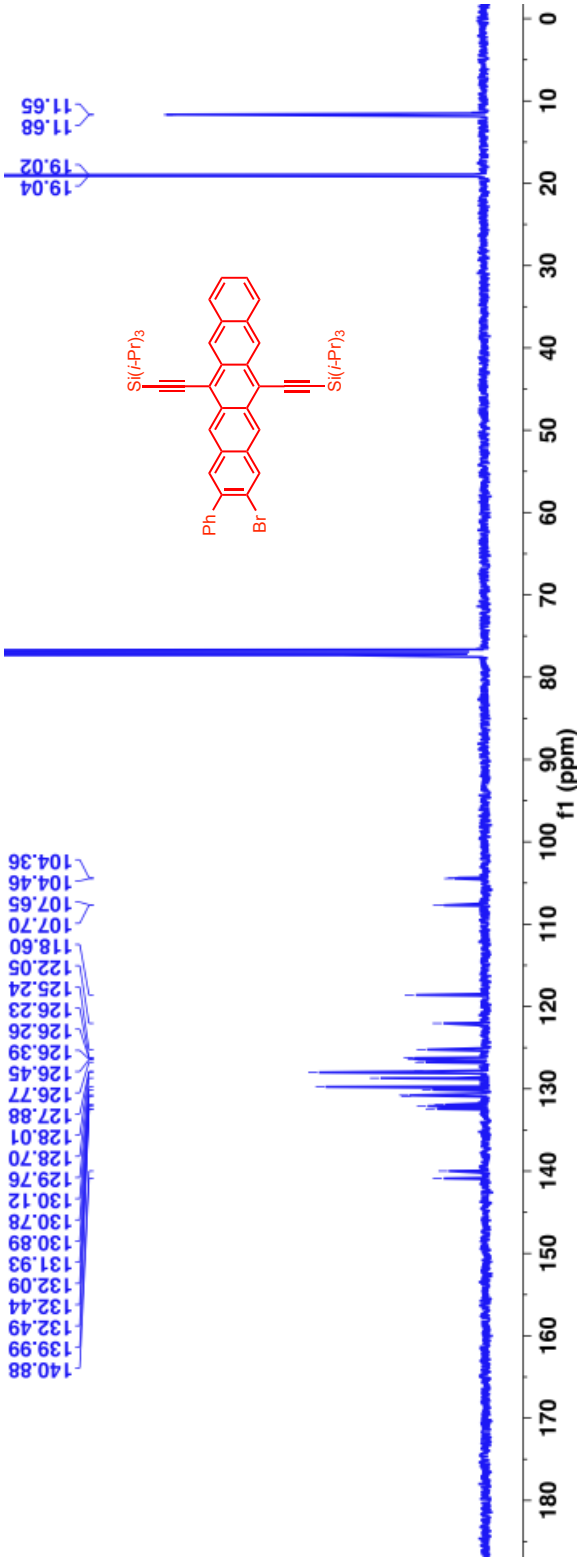

^{1}H-NMR (400 MHz, $CDCl_3$, δ ppm): 9.35 (s, 1H), 9.32-9.31 (s, 2H), 9.26 (s, 1H), 8.40 (s, 1H), 7.98-7.96 (m, 2H), 7.90-7.89 (m, 1H), 7.59-7.57 (m, 2H), 7.48-7.38 (m, 5H), 1.42-1.34 (m, 42H) and 1.29 (s, 12H).

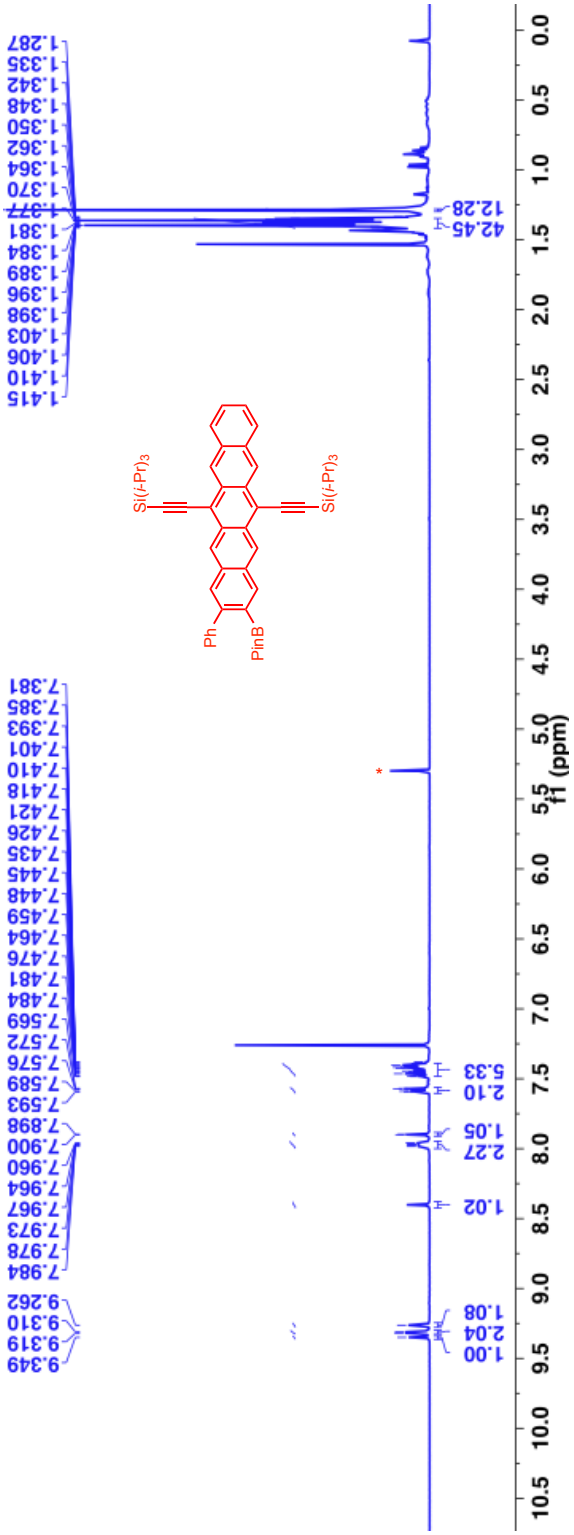

^{13}C-NMR (125 MHz, $CDCl_3$, δ ppm): 143.1, 142.7, 137.99, 132.5, 132.4, 132.3, 131.3, 130.8, 130.76, 130.7, 130.6, 129.0, 128.7, 128.0, 127.4, 127.37, 127.1, 127.0, 126.4, 126.3, 126.1, 126.06, 126.0, 118.8, 118.2, 114.9, 107.3, 107.2, 104.7, 104.6, 84.0, 24.7, 19.0, 19.02, 11.7 and 11.6.

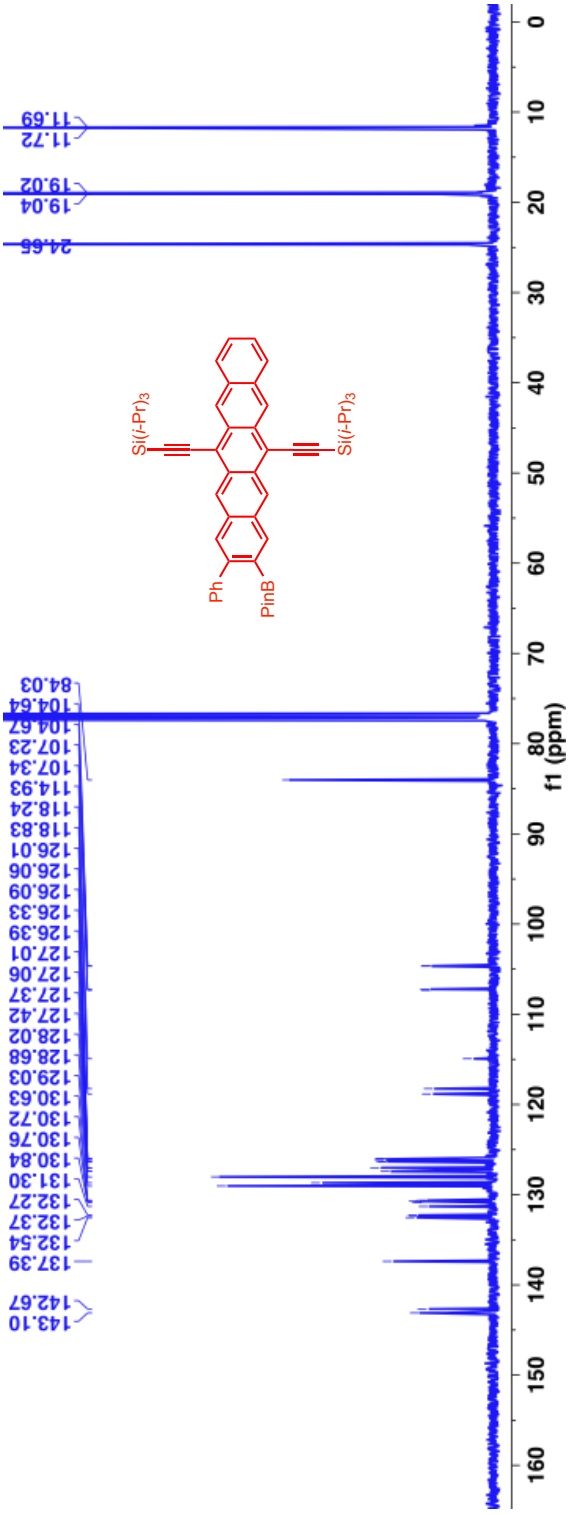

^{1}H-NMR (500 MHz, $CDCl_3$, δ ppm): 9.42 (s, 1H), 9.37 (s, 1H), 9.34-9.32 (m, 4H), 9.29 (s, 1H), 9.25 (s, 1H), 8.22 (s, 1H), 8.09-8.06 (m, 2H), 8.01-7.98 (m, 4H), 7.79-7.77 (m, 1H), 7.47-7.41 (m, 6H), 7.33-7.28 (m, 3H), 7.19-7.16 (m, 1H) and 1.46-1.35 (m, 84H).

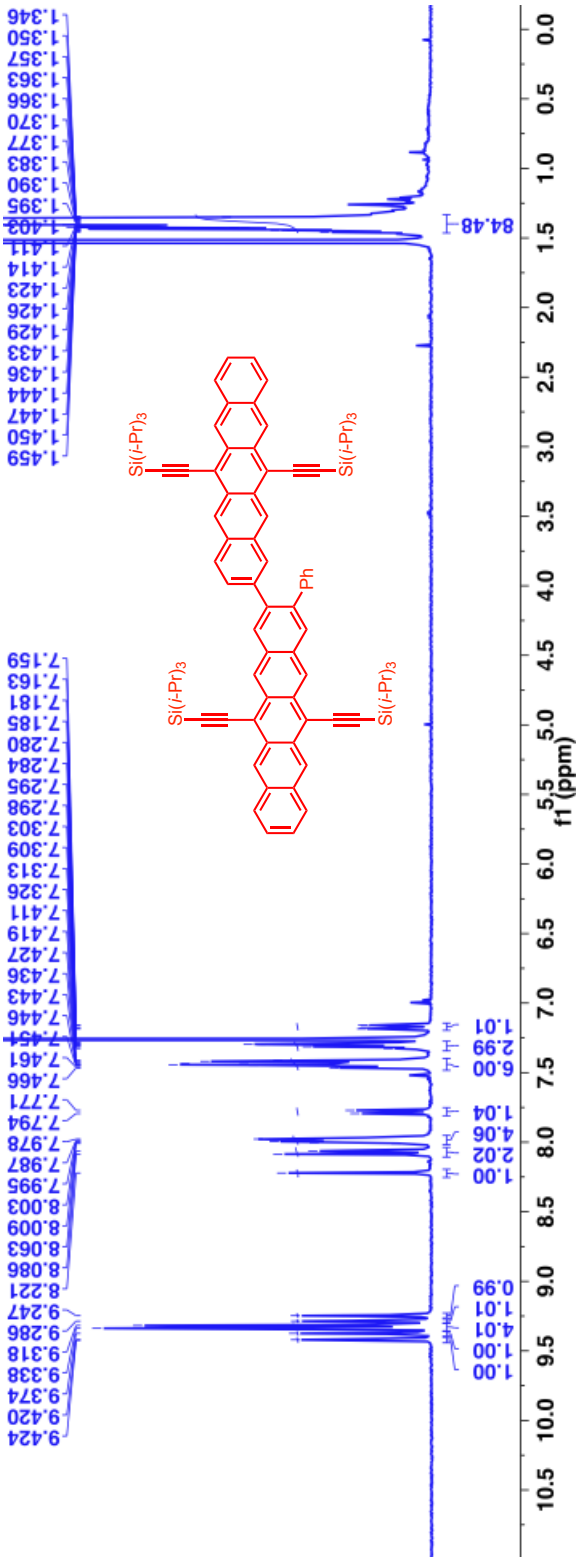

^{13}C-NMR (125 MHz, $CDCl_3$, δ ppm): 141.4, 139.8, 139.7, 139.4, 132.54, 132.53, 132.5, 132.46, 131.9, 131.87, 131.4, 131.2, 131.19, 131.0, 130.9, 130.91, 130.8, 130.78, 130.3, 130.25, 129.9, 128.9, 128.85, 128.84, 128.7, 128.4, 127.9, 127.2, 126.6, 126.58, 126.54, 126.49, 126.4, 126.3, 126.2, 118.7, 118.59, 118.56, 118.4, 107.6, 107.5, 107.4, 107.3, 104.9, 104.8, 19.19, 19.16 and 11.9.

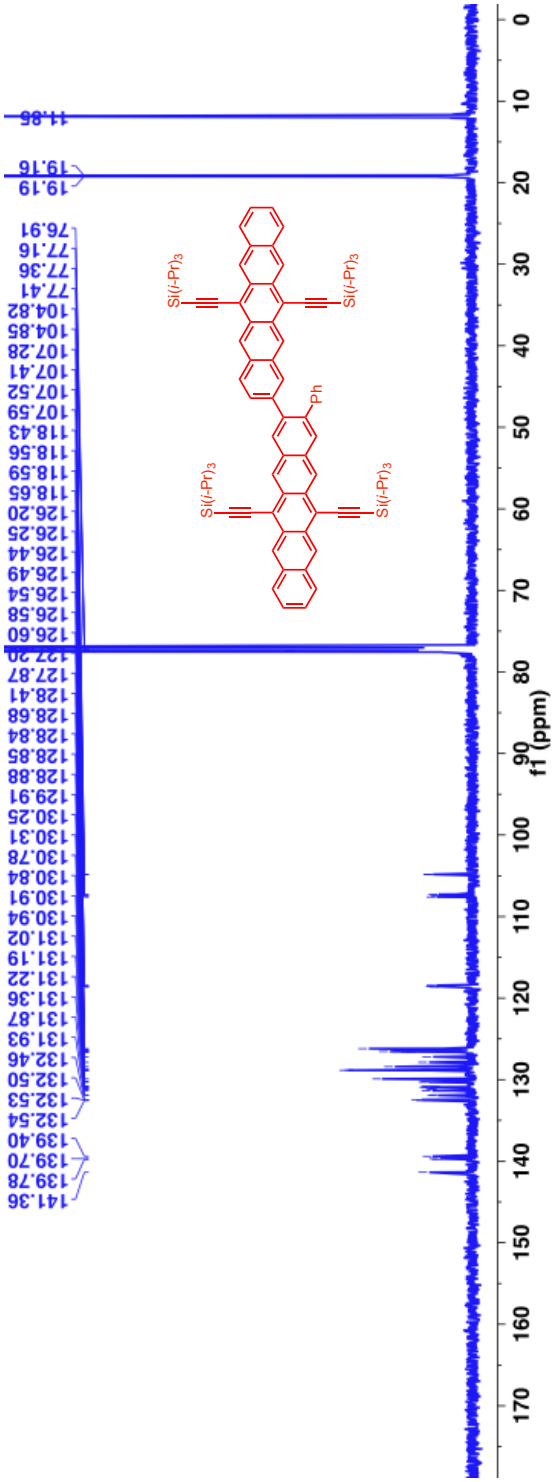

^{1}H-NMR (400 MHz, $CDCl_3$, δ ppm): 9.46 (s, 2H), 9.38-9.37 (m, 4H), 9.32 (s, 2H), 8.34 (s, 2H), 8.04-8.00 (m, 4H), 7.79 (s, 2H), 7.48-7.44 (m, 4H), 7.21-7.16 (m, 2H), 7.09-7.05 (m, 4H), 6.88-6.85 (m, 4H) and 1.47-1.37 (m, 84H).

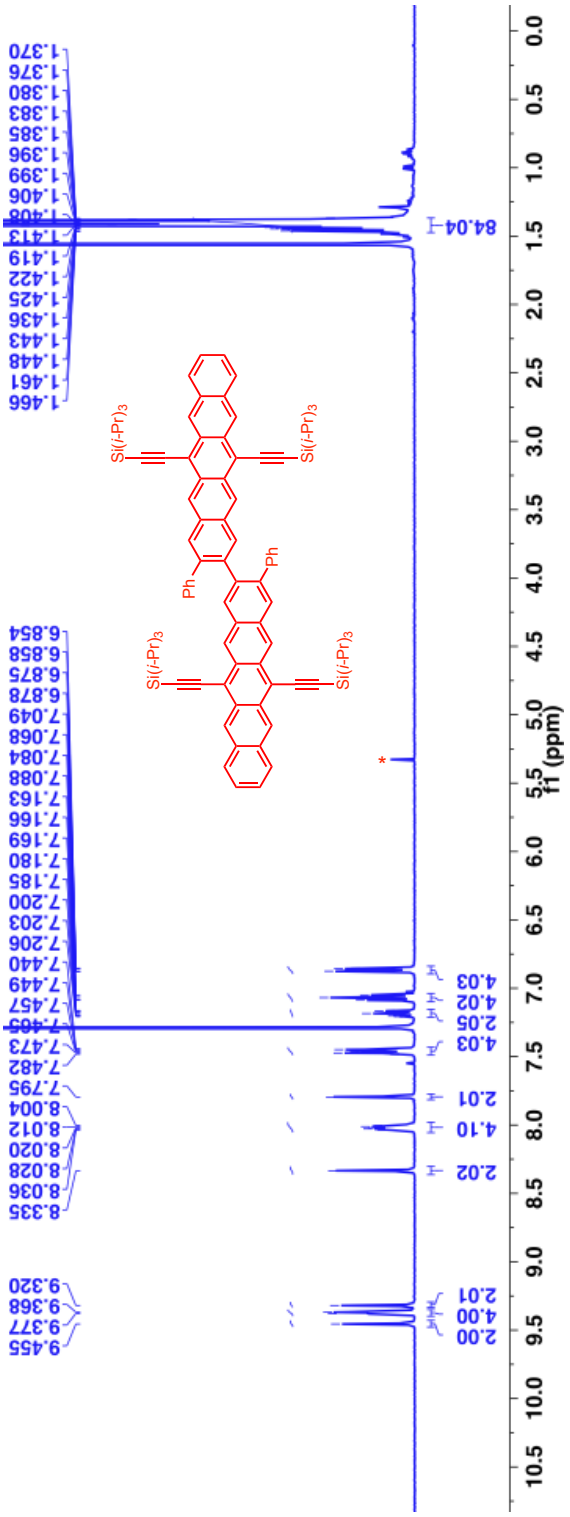

^{13}C-NMR (125 MHz, $CDCl_3$, δ ppm): 140.6, 140.2, 140.1, 132.4, 132.36, 131.99, 131.7, 131.1, 130.99, 130.95, 130.8, 130.8, 129.2, 129.1, 128.7, 127.7, 126.5, 126.4, 126.2, 126.1, 118.5, 118.4, 107.4, 107.3, 104.7, 104.67, 29.7, 19.1, 19.0, 11.7 and 11.70.

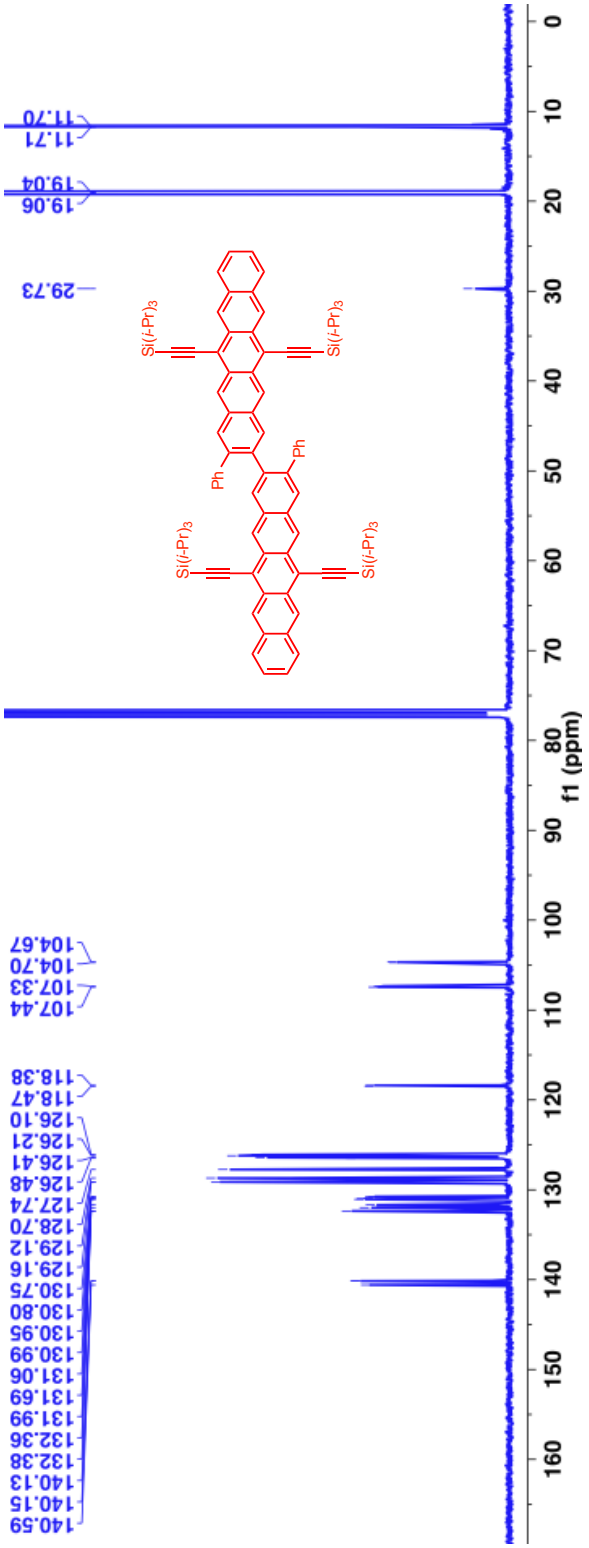

10. Supporting Information References:

(1) Snellenburg, J. J. L., S. P.; Seger, R.; Mullen, K. M.; van Stokum, I. H. M. Glotaran: A Java-Based Graphical User Interface for the R Package TIMP. *J. Stat. Soft.* **2012**, *49*, 1-22.

(2) Kaur, I.; Jia, W.; Kopreski, R. P.; Selvarasah, S.; Dokmeci, M. R.; Pramanik, C.; McGruer, N. E.; Miller, G. P. Substituent Effects in Pentacenes: Gaining Control over HOMO–LUMO Gaps and Photooxidative Resistances. *J. Am. Chem. Soc.* **2008**, *130*, 16274-16286.

(3) Becke, A. D. Density-functional thermochemistry. III. The role of exact exchange. *J. Chem. Phys.* **1993**, *98*, 5648-5652.

(4) Lee, C.; Yang, W.; Parr, R. G. Development of the Colle-Salvetti correlation-energy formula into a functional of the electron density. *Phys. Rev. B* **1988**, *37*, 785--789.

(5) Sanders, S. N.; Kumarasamy, E.; Pun, A. B.; Trinh, M. T.; Choi, B.; Xia, J.; Taffet, E. J.; Low, J. Z.; Miller, J. R.; Roy, X.; Zhu, X. Y.; Steigerwald, M. L.; Sfeir, M. Y.; Campos, L. M. Quantitative Intramolecular Singlet Fission in Bipentacenes. *J. Am. Chem. Soc.* **2015**, *137*, 8965-8972.

(6) Lukman, S.; Musser, A. J.; Chen, K.; Athanasopoulos, S.; Yong, C. K.; Zeng, Z.; Ye, Q.; Chi, C.; Hodgkiss, J. M.; Wu, J.; Friend, R. H.; Greenham, N. C. Tuneable Singlet Exciton Fission and Triplet–Triplet Annihilation in an Orthogonal Pentacene Dimer. *Adv. Funct. Mater.* **2015**, *25*, 5452-5461.

(7) Walker, B. J.; Musser, A. J.; Beljonne, D.; Friend, R. H. Singlet exciton fission in solution. *Nat. Chem.* **2013**, *5*, 1019-1024.

(8) Plunkett, K. N.; Godula, K.; Nuckolls, C.; Tremblay, N.; Whalley, A. C.; Xiao, S. Expeditious Synthesis of Contorted Hexabenzocoronenes. *Org. Lett.* **2009**, *11*, 2225-2228.

11. Coordinates For The Reference Structure Of BP-2H.

C	-6.55539	1.18082	-0.38359
C	-7.04107	-1.53091	0.38844
C	-6.31367	2.53042	-0.76782
C	-7.28280	-2.88052	0.77266
C	-6.10780	3.67983	-1.09506
C	-7.48866	-4.02994	1.09989
H	-5.92675	4.69068	-1.38284
H	-7.66970	-5.04077	1.38768
C	-7.88553	0.67453	-0.38910
C	-5.46434	0.35220	0.00197
C	-8.13211	-0.70230	0.00287

C	-5.71095	-1.02461	0.39395
C	-8.98354	1.47780	-0.76775
C	-4.13642	0.83254	0.01517
C	-9.46005	-1.18262	-0.01032
C	-4.61290	-1.82789	0.77259
H	-8.79699	2.50669	-1.06040
H	-3.95431	1.86204	-0.27819
H	-9.64214	-2.21212	0.28305
H	-4.79948	-2.85678	1.06524
C	-10.28708	0.99339	-0.77675
C	-3.06308	0.03172	0.39008
C	-10.53338	-0.38180	-0.38524
C	-3.30938	-1.34347	0.78158
C	-11.40416	1.80786	-1.16112
C	-1.71306	0.51776	0.40421
C	-11.88339	-0.86786	-0.39937
C	-2.19231	-2.15794	1.16598
H	-11.21621	2.83829	-1.45409
H	-1.53172	1.54908	0.11018
H	-12.06474	-1.89917	-0.10534
H	-2.38024	-3.18838	1.45893
C	-12.67428	1.30248	-1.15966
C	-0.67893	-0.29436	0.77783
C	-12.91752	-0.05573	-0.77299
C	-0.92220	-1.65256	1.16453
H	-13.51251	1.92907	-1.45283
H	-13.93596	-0.43516	-0.77973

H	-0.08395	-2.27915	1.45767
C	6.55538	-1.18081	-0.38359
C	7.04107	1.53090	0.38844
C	6.31367	-2.53042	-0.76781
C	7.28280	2.88052	0.77266
C	6.10780	-3.67984	-1.09506
C	7.48866	4.02994	1.09989
H	5.92675	-4.69069	-1.38284
H	7.66971	5.04078	1.38768
C	7.88552	-0.67453	-0.38910
C	5.46434	-0.35221	0.00197
C	8.13211	0.70231	0.00287
C	5.71094	1.02461	0.39395
C	8.98354	-1.47780	-0.76775
C	4.13642	-0.83255	0.01517
C	9.46005	1.18263	-0.01033
C	4.61290	1.82789	0.77259
H	8.79699	-2.50670	-1.06040
H	3.95431	-1.86203	-0.27819
H	9.64214	2.21212	0.28305
H	4.79948	2.85679	1.06524
C	10.28708	-0.99339	-0.77675
C	3.06308	-0.03172	0.39008
C	10.53338	0.38180	-0.38524
C	3.30939	1.34347	0.78158
C	11.40417	-1.80787	-1.16112
C	1.71306	-0.51776	0.40420

C	11.88340	0.86786	-0.39937
C	2.19231	2.15795	1.16597
H	11.21622	-2.83830	-1.45409
H	1.53172	-1.54909	0.11018
H	12.06474	1.89918	-0.10534
H	2.38024	3.18839	1.45893
C	12.67427	-1.30248	-1.15966
C	0.67893	0.29436	0.77783
C	12.91752	0.05573	-0.77299
C	0.92220	1.65256	1.16453
H	13.51251	-1.92907	-1.45282
H	13.93596	0.43516	-0.77974
H	0.08395	2.27915	1.45767

12. Optimized S_1 Structure Of The Truncated TIPS-Pentacene Monomer.

C	0.00000000	1.42927015	0.00000000
C	0.00000000	-1.42927015	0.00000000
C	0.00000000	2.84705758	0.00000000
C	0.00000000	-2.84705758	0.00000000
C	0.00000000	4.06055307	0.00000000
C	0.00000000	-4.06055307	0.00000000
H	0.00000000	5.12811708	0.00000000
H	0.00000000	-5.12811708	0.00000000
C	1.24618638	0.72458410	0.00000000
C	-1.24618638	0.72458410	0.00000000
C	1.24618638	-0.72458410	0.00000000
C	-1.24618638	-0.72458410	0.00000000

C	2.47300339	1.39509976	0.00000000
C	-2.47300339	1.39509976	0.00000000
C	2.47300339	-1.39509976	0.00000000
C	-2.47300339	-1.39509976	0.00000000
H	2.47154498	2.48253703	0.00000000
H	-2.47154498	2.48253703	0.00000000
H	2.47154498	-2.48253703	0.00000000
H	-2.47154498	-2.48253703	0.00000000
C	3.71313381	0.71891922	0.00000000
C	-3.71313381	0.71891922	0.00000000
C	3.71313381	-0.71891922	0.00000000
C	-3.71313381	-0.71891922	0.00000000
C	4.95171928	1.40184164	0.00000000
C	-4.95171928	1.40184164	0.00000000
C	4.95171928	-1.40184164	0.00000000
C	-4.95171928	-1.40184164	0.00000000
H	4.94953203	2.49046826	0.00000000
H	-4.94953203	2.49046826	0.00000000
H	4.94953203	-2.49046826	0.00000000
H	-4.94953203	-2.49046826	0.00000000
C	6.14844370	0.70437098	0.00000000
C	-6.14844370	0.70437098	0.00000000
C	6.14844370	-0.70437098	0.00000000
C	-6.14844370	-0.70437098	0.00000000
H	7.09218216	1.24478328	0.00000000
H	-7.09218216	1.24478328	0.00000000
H	7.09218216	-1.24478328	0.00000000

H -7.09218216 -1.24478328 0.00000000

13. Optimized T_1 Structure Of The Truncated TIPS-Pentacene Monomer.

C	0.00000000	1.43657625	0.00000000
C	0.00000000	-1.43657625	0.00000000
C	0.00000000	2.84920144	0.00000000
C	0.00000000	-2.84920144	0.00000000
C	0.00000000	4.06490421	0.00000000
C	0.00000000	-4.06490421	0.00000000
H	0.00000000	5.13127995	0.00000000
H	0.00000000	-5.13127995	0.00000000
C	1.25642908	0.72565770	0.00000000
C	-1.25642908	0.72565770	0.00000000
C	1.25642908	-0.72565770	0.00000000
C	-1.25642908	-0.72565770	0.00000000
C	2.47491884	1.39652407	0.00000000
C	-2.47491884	1.39652407	0.00000000
C	2.47491884	-1.39652407	0.00000000
C	-2.47491884	-1.39652407	0.00000000
H	2.47517848	2.48266292	0.00000000
H	-2.47517848	2.48266292	0.00000000
H	2.47517848	-2.48266292	0.00000000
H	-2.47517848	-2.48266292	0.00000000
C	3.72162890	0.71660829	0.00000000
C	-3.72162890	0.71660829	0.00000000
C	3.72162890	-0.71660829	0.00000000
C	-3.72162890	-0.71660829	0.00000000
C	4.95959187	1.40299916	0.00000000

C	-4.95959187	1.40299916	0.00000000
C	4.95959187	-1.40299916	0.00000000
C	-4.95959187	-1.40299916	0.00000000
H	4.95702934	2.49070835	0.00000000
H	-4.95702934	2.49070835	0.00000000
H	4.95702934	-2.49070835	0.00000000
H	-4.95702934	-2.49070835	0.00000000
C	6.15538931	0.70583850	0.00000000
C	-6.15538931	0.70583850	0.00000000
C	6.15538931	-0.70583850	0.00000000
C	-6.15538931	-0.70583850	0.00000000
H	7.09895086	1.24505115	0.00000000
H	-7.09895086	1.24505115	0.00000000
H	7.09895086	-1.24505115	0.00000000
H	-7.09895086	-1.24505115	0.00000000